Measurement and Interpretation of Neutron Total Cross Sections of Carbon, Calcium, and Lead*

R. M. WILENZICK, G. E. MITCHELL,† K. K. SETH, AND H. W. LEWIS
Duke University, Durham, North Carolina

(Received August 29, 1960)

The neutron total cross sections of carbon, calcium, and lead have been determined in the energy region 200–960 kev using a time-of-flight technique. The observed cross section for carbon has been analyzed in terms of the effective-range theory as well as the bound-level contribution, with results which agree very well with those obtained by the (d,p) stripping experiments. Also it is concluded that the upper limit for the total width of the "proposed" resonance in C^{13} at 610 kev is 100 ev. For calcium and lead the data are analyzed for resonance parameters. It is found that the s-wave strength function for Ca^{40} increases rapidly with increasing energy. It is concluded also that the course of the Pb cross sections can be explained only by the presence of a broad s-wave resonance in Pb^{208}, at $E_n=515\pm15$ kev with a neutron width $\Gamma_n=100\pm15$ kev.

INTRODUCTION

THE total cross sections of carbon, calcium, and lead are of special importance. All these nuclei are even-even and calcium and lead are doubly magic. Further, the extensive use of these elements in shielding and in other aspects of nuclear technology makes a careful investigation important. Previous measurements[1] have been made with an average resolution of about 10–30 kev in the energy region 200 kev to 1 Mev. The present experiments were performed with an average resolution of ~5 kev in order to study more of the details of the resonance structure in C, Ca, natural Pb, and radio-lead, and a more detailed analysis of the data has been made.

Cranberg, Beauchamp, and Levin[2] have discussed the advantages of using an organic scintillator and a time-of-flight system in the measurement of neutron total cross sections. The neutrons in the forward direction from the $Li^7(p,n)Be^7$ reaction cease to be monoenergetic when the main group reaches an energy of ~650 kev. The time-of-flight system discriminates against both the unwanted group and the background and provides a higher counting rate than a "long counter" placed far from the target. A time resolution of 10 mμsec and a flight path two feet long enable one to resolve the two neutron groups up to an energy of 1.0 Mev for the main group.

The experiments reported here were done using the Duke University time-of-flight apparatus. We present a brief description of the apparatus and the results of the analysis of the data obtained.

APPARATUS

Protons from the Duke 4-Mev Van de Graaff accelerator passed through an electrostatic analyzer[3] whose slits were adjusted for a proton beam resolution of 1 part in 1500. The beam was then swept across a slit in front of the Li target by applying a 4-Mc voltage between two parallel plates located near the exit slits of the electrostatic analyzer. The burst width so obtained was about 5 mμsec.

The Li target was evaporated on a nickel end cap soldered to a stainless steel Faraday cup, and attached to the beam tube by means of a glass pipe. The effective resolution was determined by the setting of the electrostatic analyzer and the Li target thickness. It was varied for different elements to provide the required resolution.

In order to maximize the beam emerging from the exit slits of the electrostatic analyzer, the "homogenizer,"[4] which reduces time-dependent components of the energy spread, was employed. The average beam at the target was about 0.2 μa.

The detector arrangement was very similar to that used by Cranberg *et al.*[2] The 2-in.×2-in. "Sintilon" plastic scintillator (manufactured by National Radiac Corporation, Newark, New Jersey) was located 24 in. from the target and was viewed by two RCA-6342 photomultipliers in coincidence. It was surrounded by a $\frac{3}{16}$-in. lead shield. The neutron collimator was composed of a mixture of Li_2CO_3 and paraffin.

The samples, in the form of disks 1 to 2 inches diameter, were mounted on a sample changer and placed midway between the target and the detector. Usually two different sample thicknesses were used.

The time-to-pulse-height convertor was essentially the same as that developed by Weber, Johnstone, and Cranberg.[5] A ten-channel pulse-height analyzer of the Los Alamos design was used. The over-all resolution of the time-of-flight neutron peak, as displayed in the 10-channel analyzer, was ~10 mμsec. The neutron beam was monitored by a BF_3 "long counter" placed at 60° at a distance of 2 ft from the target.

* This work was supported by the U. S. Atomic Energy Commission.

† Now at Florida State University, Tallahassee, Florida.

[1] D. J. Hughes, B. A. Magurno, and M. K. Brussel, *Neutron Cross Sections*, Brookhaven National Laboratory Report, BNL-325 (Superintendent of Documents, U. S. Government Printing Office, Washington, D. C., 1960), 2nd ed., Suppl. No. 1.

[2] L. Cranberg, R. K. Beauchamp, and J. S. Levin, Rev. Sci. Instr. 28, 89 (1957).

[3] A. L. Toller, Ph.D. thesis, Duke University, 1954 (unpublished).

[4] P. B. Parks, H. W. Newson, and R. M. Williamson, Rev. Sci. Instr. 29, 834 (1958).

[5] W. Weber, C. W. Johnstone, and L. Cranberg, Rev. Sci. Instr. 27, 166 (1956).

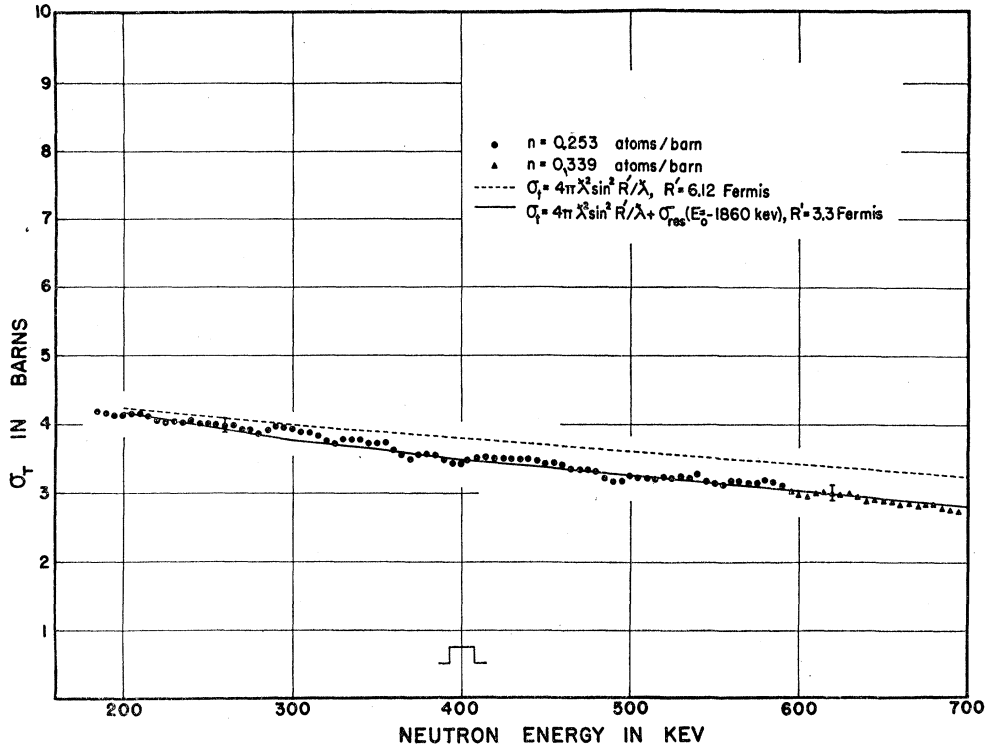

FIG. 1. σ_t for carbon (natural). The dashed line is the best fit assuming σ_t is solely due to shape-elastic scattering, $R'=\rho_0 A^{\frac{1}{3}}$, $\rho_0=2.67$ fermis. The solid line is the best fit assuming an s-wave bound level at $E_0=-1.86$ Mev, and with $\gamma_\lambda^2=1.75$ Mev and $R'=3.3$ fermis or $\rho_0=1.45$ fermis. The fit due to the effective-range analysis discussed in the text corresponds to $\gamma_\lambda^2=1.72$ Mev and is indistinguishable from the solid line shown. Note the absence of resonance structure in the neighborhood of $E_n=600$ kev.

The absolute energy of the proton beam was determined by the setting of the electrostatic analyzer, which was calibrated by determining the forward threshold for neutron production. The neutron energy spread varied from 3 kev at 200 kev to 7 kev at 900 kev. At a given proton energy, the neutron peak was centered in the ten-channel analyzer with and without the sample intercepting the neutron beam. The ratio of the areas under these peaks gave the transmission. The smooth background due to gamma rays and stray neutrons was not included in these areas.

RESULTS

Carbon

Figure 1 shows the observed cross section of carbon in the neutron energy range 180 kev to 700 kev. A sample of thickness $n=0.253$ atom/barn was used in the region 180 kev to 590 kev and another of $n=0.339$ atom/barn in the region 595–700 kev. No indication of the shallow dip indicated by the data of Bretscher *et al.*[6] in the energy region 200 kev to 400 kev was found; neither was any resonance structure revealed in the neighborhood of 610 kev corresponding to the position of a level in C^{13} found in the study of $B^{11}(He^3,p)C^{13}$ reaction by Moak *et al.*[7] The maximum deviation of our measured cross section is 0.2 barn, which yields an upper limit $\Gamma_n \lesssim 100$ ev for the width of the resonance in question. The standard deviation of our data is ~0.1 barn, consistent with the counting statistics, and in itself would mask levels with $\Gamma_n \lesssim 70$ ev. We therefore conclude that $\Gamma_n \lesssim 100$ ev for the suspected $f_{\frac{5}{2}}$ level in the neighborhood of 600 kev.

The absolute values of our cross sections are in excellent agreement with those reported by Huddleston, Lane, Lee, and Mooring.[8] It is of interest to attempt an interpretation of this structureless cross section in terms of our knowledge of the compound nucleus C^{13}. The first such attempt was made by Thomas[9] who had available relatively inaccurate cross sections. The fact that the neutron energy region 0–1 Mev is far removed from both bound and virtual levels makes it particularly suitable for an effective-range type analysis. An alternative approach is to try to subtract the contribution of all the known bound and virtual levels and attempt to fit the remaining cross section in terms of the hard-sphere scattering of the form $4\pi\lambda^2 \sin^2(R'/\lambda)$.

At this stage let us review the information about the levels in the compound nucleus C^{13}. Figure 2, which is

[6] E. Bretscher and E. B. Martin, Helv. Phys. Acta **23**, 15 (1950).
[7] C. D. Moak, A. Galonsky, R. L. Traughber, and C. M. Jones, Phys. Rev. **110**, 1369 (1958).
[8] C. M. Huddleston, R. O. Lane, L. L. Lee, Jr., and F. P. Mooring, Argonne National Laboratory Report ANL-6111, February, 1960 (unpublished).
[9] R. G. Thomas, Phys. Rev. **88**, 1109 (1952).

based on Ajzenberg-Selove and Lauritsen,[10] shows the level structure of C^{13}. The bound p- and d-wave levels can hardly affect the course of neutron cross sections of C^{12}. As a matter of fact if we assume the widths as determined by (d,p) experiments,[10] the total contribution due to bound levels at -4.95 ($g.s.$), -1.27 and -1.10 Mev is $\leqslant 0.1$ barn. Similarly the contribution of all known virtual levels is found to be $\leqslant 0.1$ barn and is of opposite sign. Thus the level which could possibly be held responsible for the course of the total cross sections of C^{12} must be the one at -1.86 Mev. From (d,p) experiments it is known that its angular momentum $l=0$, and an estimate of its width is also available.[11] We shall, however, not assume this information and show that the same results are obtained from our analysis of the C^{12} neutron total cross sections.

An effective-range analysis of our cross section was made. We know that

$$k\cot\delta_0=-[(4\pi/\sigma_t)-k^2]^{\frac{1}{2}}$$
$$=-\alpha+\tfrac{1}{2}k^2r_0-Pk^4r_0^3+\cdots, \quad (1)$$

where $1/\alpha$ is the *scattering length*, r_0 is the *effective range* and P is the *shape factor* for the nuclear potential. A least-squares fit of $(k\cot\delta_0)$ to the above polynomial resulted into two different fits which must be considered equally good since their rms errors differ by an amount much less than the error in our measured cross sections. The parameters for both these fits are listed in Table I. It is difficult to decide in favor of either of these fits simply by "goodness of fit" criterion. Accurate determination of cross sections at lower energy would perhaps lead to the choice between the two. The zero-energy cross section reported in the literature[12] is 4.7 ± 0.2 barns, which would decide in favor of the fit (a). However, Walton *et al.*[13] have recently reported measurements which indicate $\sigma_t(E=0)=5.2\pm0.2$. Seth *et al.*[14] also find that $\sigma_t=5.1\pm0.2$ at $E_n=5$ kev. Both these experiments would tend to favor fit (b). The value 0.297 for the shape factor in fit (a) is too large and corresponds to an extremely long-tailed exponential-like potential which is very unlikely, while fit (b) corresponds to a potential shape very close to a square well. Fit (b) also agrees with the following simple rule which is strictly true only for a square well potential of depth V_0 and radius R: For usual values of $V_0\rho_0^2$ ($\sim$50 Mev fermi^2),

$$\tfrac{2}{3}R\leqslant r_0\leqslant R.$$

As shown later in this section, we find that $R\approx R'=3.3$ fermis so that $2.2\leqslant r_0\leqslant 3.3$ fermis. On the basis of this rule, fit (b) is preferred since $r_0=2.62$ fermis for fit (b) while it is equal to 3.64 fermis for fit (a). The predicted cross section curve for this fit is not shown in Fig. 1 because it is indistinguishable from the solid curve, which is based on independent considerations described below. The fit to the experimental data is gratifying.

From the above effective-range analysis it is possible to derive an estimate of $\gamma_\lambda^2/E_\lambda$ of the bound level[15] which is primarily responsible for the observed cross section. According to Lane and Thomas,[16] the $\mathcal{R}$ function at "zero" energy is

$$\mathcal{R}(E=0)=\mathcal{R}^{(0)}=1-[1/(\alpha R)]. \quad (2)$$

If now the contribution to the $\mathcal{R}$ function is primarily due to one level, then

$$\mathcal{R}(E=0)=\textstyle\sum_\lambda(\gamma_\lambda^2/E_\lambda)\simeq(\gamma_\lambda^2/E_\lambda)_{\text{single level}}. \quad (3)$$

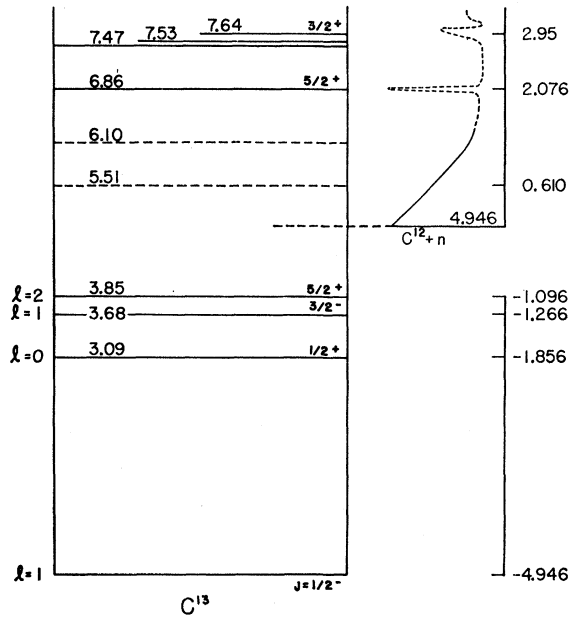

FIG. 2. Level structure for the compound nucleus C^{13}.

TABLE I. Results of effective range analysis of σ_t for C^{12} in the energy range 180 kev to 700 kev.

Fit	Rms error[a]	$1/\alpha$ Scattering length (fermis)	r_0 Effective range (fermis)	P Shape factor	Zero-energy σ_t as predicted by the fit (barns)
(a)	0.051	6.203	3.638	+0.297	4.836
(b)	0.055	6.360	2.620	0	5.082

[a] Rms error for a polynomial fit is defined as $\{[\Sigma(y_d-y_c)^2]/\Sigma y_d^2\}^{\frac{1}{2}}$, where y_d is the given value of y in the data and y_c is the value calculated from the polynomial.

[10] F. Ajzenberg-Selove and T. Lauritsen, Nuclear Phys. **11**, 1 (1959).
[11] M. T. McEllistrem, Phys. Rev. **111**, 596 (1958).
[12] W. W. Havens, Jr., and L. J. Rainwater, Phys. Rev. **75**, 1296 (1949).
[13] R. B. Walton, N. F. Wikner, J. L. Wood, and J. R. Beyster, Bull. Am. Phys. Soc. 4, 288 (1960).
[14] K. K. Seth, E. G. Bilpuch, and H. W. Newson (unpublished).
[15] We shall be using γ_λ^2, $\Gamma_n^{(l)}$, and Γ interchangeably in this paper. It is worthwhile to define their relationship here:

$$\Gamma_n^{(l)}=\Gamma_n v_l^{-1}\{1(\text{ev})/E(\text{ev})\}^{\frac{1}{2}}$$
$$=0.4394\gamma^2R\times10^{-3},$$
$$(\Gamma_n^{(l)})_{s.p.}\simeq27\times10^3/R,$$

where R is in fermis, and $\Gamma_n^{(l)}$, γ^2, and Γ_n are in ev.
[16] A. M. Lane and R. G. Thomas, Revs. Modern Phys. **30**, 257 (1958).

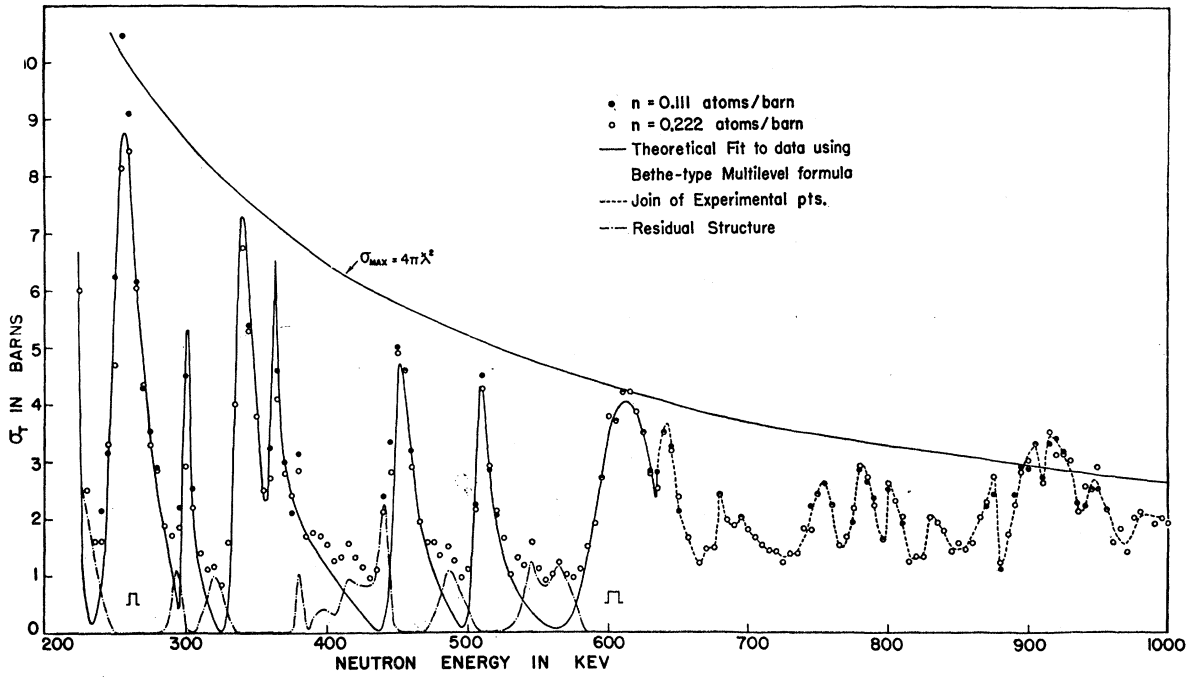

FIG. 3. σ_t for calcium (natural). The solid line shows the best fit obtained by a Bethe-type multilevel formula with parameters as listed in Table II. $R'=4.0$ fermis was assumed. The dashed line is the difference $\sigma_t(\text{obs})-\sigma_t(\text{calculated})$ and indicates unresolved levels, perhaps due to higher angular momenta and/or minor isotopes.

Equating (2) and (3), we get

$$\begin{aligned}\gamma_\lambda^2 &= E_\lambda[1-(1/\alpha R)]\\ &= -0.89E_\lambda \quad \text{for fit } (a)\\ &= -0.93E_\lambda \quad \text{for fit } (b).\end{aligned} \tag{4}$$

If the level at 3.09 Mev ($E_\lambda=-1.86$ Mev) is the level in question, this leads to

$$\begin{aligned}\gamma_\lambda^2 &= 1.66 \text{ Mev for fit } (a), \quad \text{or}\\ &= 1.72 \text{ Mev for fit } (b).\end{aligned} \tag{5}$$

As mentioned earlier, an alternative method of analysis is to fit the observed $\sigma_t=\sigma_{\text{pot}}+\sigma_{\text{res}}$. Figure 1 shows such attempts. The dashed line is the best fit if it is assumed that the observed cross section is wholly due to potential scattering. The fit is poor and gets worse at higher energy. Further, $R'=\rho_0 A^{\frac{1}{3}}=6.12$ fermis is required, corresponding to $\rho_0=2.67$ fermis, which is too large. We must therefore consider resonance contributions due to all levels. As mentioned above, the net contribution due to levels other than the one at -1.86 Mev is $\ll 0.1$ barn. An attempt was made therefore to fit the observed σ_t with potential scattering cross section plus the total cross section due to a level at -1.86 Mev.

$$\sigma_t=4\pi\lambda^2\sin^2\alpha+[\sigma_0/(1+x^2)][\cos 2\alpha+x\sin 2\alpha], \tag{6}$$

where $\sigma_0=4\pi\lambda^2 g(\Gamma_n/\Gamma)$; $x=2(E-E_0)/\Gamma$; $\alpha=$potential phase shift, $=R'/\lambda$ for $l=0$; $g=$the statistical weight factor. All attempts to fit the observed σ_t assuming that this level could be $l\geqslant 1$ were unsuccessful. It was therefore assumed that $l=0$ and fits were attempted treating R' and $\Gamma=\Gamma_n$ as free parameters. The visual best fit obtained after a number of trials is shown in Fig. 1. The parameters for this fit are

$$R'=3.3 \text{ fermis}, \ \Gamma_n^0=2.54 \text{ kev, i.e., } \gamma_\lambda^2=1.75 \text{ Mev}. \tag{6}$$

It may be noticed that this result is in excellent agreement with the independent result of the effective-range analysis [Eq. (5)] and favors fit (b) of Table I.

Calcium

The total cross section of calcium was measured from 200 kev to 1000 kev and is shown in Fig. 3. The entire energy range was covered with two sample thicknesses having $n=0.111$ and $n=0.222$ atom/barn. The two samples yielded almost identical results, with the thicker sample showing less point scatter in the low cross-section regions and the thinner sample giving slightly higher peak cross sections.

Seven prominent resonances were observed in the energy region 230 to 630 kev. Area analysis[17] of these resonances for the two sample thicknesses yielded widths as shown in Column 2 of Table II. These resonances were all assigned to $l=0$ neutrons on the basis of consistency between thin- and thick-sample results and shape considerations.[17] For example, the resonance at 595 kev has an observed width of about 50 kev. Area analysis yields $\Gamma_n(l=0,\ g=1)=70\pm 15$ kev, $\Gamma_n(l=1,\ g=1)=17\pm 4$ kev, $\Gamma_n(l=1,\ g=2)=9\pm 2$ kev.

[17] Kamal K. Seth, Ann. Phys. 8, 223 (1959).

TABLE II. Resonance parameters for Ca^{40}.

E_0 (kev)	Γ_n [a] (kev)	Γ_n [b] (kev)	Γ_n^0 [c] (ev)	$10^3\times\gamma\lambda^2/(\gamma^2)_{s.p.}$ [d]
88[e]		0.148[e]	0.5	0.099
132[e]		2.54[e]	7.0	1.289
144[e]		0.190[e]	0.5	0.094
167[e]		2.49[e]	6.1	1.120
222[e]		5.65[e]	12.0	2.204
254±1	21±2	22.7±2	45.0±5.0	8.264
299±2	3±2	2.19±0.5	4.0±1.0	0.900
337.5±1	15.5±2	13.65±1.2	23.5±2.0	4.316
360±2	3±2	1.5±0.6	2.5±1.0	0.459
447.5±2	15±3	13.38±1.5	20.0±2.0	3.673
504±2	13±3	10.65±2.0	15.0±3.0	2.754
595±2	70±15	57.86±4.0	75.0±5.0	13.774

[a] The values of Γ_n listed in this column are those obtained by area analysis of the resonances.
[b] The values of Γ_n listed in this column are as obtained for the best multilevel fit to the data. Note that in all cases these values lie within the quoted uncertainty of the results of area analysis in the previous column.
[c] The values of Γ_n^0 correspond to the best fit values of Γ_n in the last column.
[d] $(\gamma^2)_{s.p.}$ denotes single-particle limit or Wigner limit of the reduced width. The entries therefore correspond to ratio of observed reduced width to the Wigner limit.
[e] The parameters for these resonances are from reference 19.

Obviously unless the resolution were of the order of 50 kev, the resonance cannot be ascribed to p-wave neutrons. Since the known experimental resolution was about 7 kev at 600 kev, the resonance must be due to $l=0$ neutrons. As a further check the parameters so obtained were fed into a Bethe-type multilevel formula:

$$\sigma_t=4\pi\lambda^2|\sum[A_{\rm res}(\Gamma_n)]+A_{\rm pot}(R')|^2.$$

While this formula is known to be relatively inaccurate at peaks, it was found that it represents a considerable improvement over the single-level Breit-Wigner formula. The computation was done on an IBM-650 computer and parameters were varied while the best fit was obtained. The final values of Γ_n^0 are listed in Column 4 of Table II. It was also found that the value of R' required by a single-level-type analysis was not the same as that which gave the best fit with the multilevel expression. The best value of R' was found to be 4.0 fermis.

In Fig. 3 the solid curve is the best multilevel fit to the data for the parameters given in Column 4 of Table II. No attempt was made to analyze levels above $E_n=630$ kev. It may be noticed that in spite of the inadequacies of the multilevel formula and the experimental resolution, an excellent fit is obtained for all the resonances analyzed. In the region between resonances the fit is relatively poor. While this may be due to the inability of the Bethe-type multilevel expression to account for level-level interference correctly, it may be due in part to the presence of narrow resonances with $l\geqslant 0$ in these regions. A number of these "resonances," labeled as "residual structure" and drawn by dashed lines in Fig. 3 are indicated in the recent high resolution work of Bowman.[18] From the present work,

[18] C. D. Bowman, Ph.D. thesis, Duke University, 1961 (unpublished).

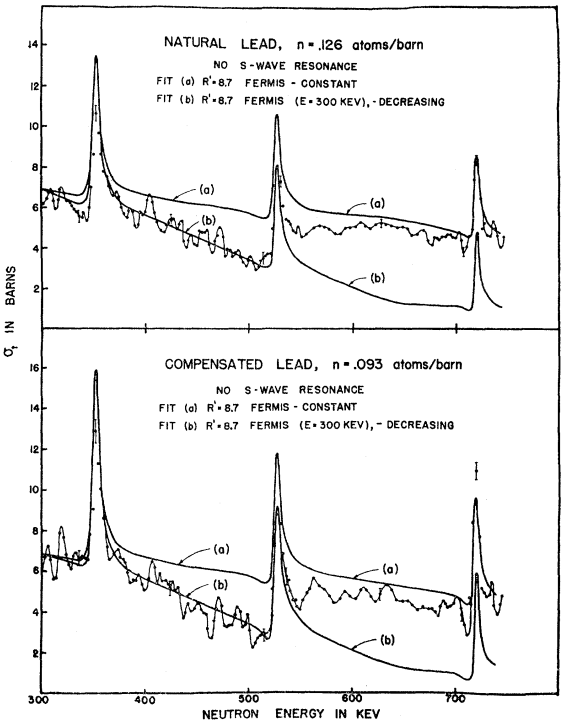

FIG. 4. σ_t for natural and compensated (for Pb^{206}) lead. The calculated fits marked (a) correspond to the assumption that R' is constant over the energy interval and only p-wave resonances 1, 3, and 4 of Table III exist, with parameters as shown in that table. Curves (b) correspond to the same resonances as for curves (a), but with an R' which decreases rapidly with energy so as to yield the shape of the observed cross sections in the energy region 380 to 520 kev. Note that fits (a) are poor in the region 380 to 520 kev and fits (b) are poor in the region 560 to 700 kev.

however, the existence of these resonances must be regarded as tentative, with the possible exception of those at 440 kev and 485 kev.

Lead

A sample of natural lead (Pb^{208} 52%, Pb^{207} 21%, Pb^{206} 26%) with thickness $n=0.126$ atom/barn, as well as a sample of radio-lead (Pb^{208} 3%, Pb^{207} 9%, Pb^{206} 88%) with thickness $n=0.0339$ atom/barn, were studied over the energy range 300 to 740 kev. The radio-lead sample was too thin to give accurate cross sections of Pb^{206} by itself, but it served as an accurate compensator for the Pb^{208} sample. Thus if I_N, I_R, and I_0 denote the number of counts with the natural lead sample in, with the radio lead sample in, and with the open beam, then while $T_1=I_N/I_0$ gives the transmission due to natural lead, $T_2=I_N/I_R$ gives the transmission due to compensated lead (effective percentage-Pb^{208} 70%, Pb^{207} 28%, Pb^{206} 0%, Pb^{204} 2%).

These cross sections are shown in Figs. 4 and 5. It is obvious that besides the three prominent resonances at $E_n=352$ kev, 526 kev, and 718 kev, there are a number of other small resonances, e.g., those at 305, 320, 375, 405, 475 kev, etc. From simple peak height considera-

tions it follows that if we limit ourselves to s-, p-, and d-wave resonances the three large resonances must be in Pb^{208}. Also we find that the ratio $\varrho=(\sigma_{max}-\sigma_{min})_{c.l.}/(\sigma_{max}-\sigma_{min})_{n.l.}$, where c.l. and n.l. refer to compensated lead and natural lead, respectively, is approximately 1.3 which is the same as the ratio between the fractional content of Pb^{208} in the compensated lead and the fractional content of Pb^{208} in the natural sample.

Both natural lead and compensated lead samples still contain Pb^{207}($\sim$25%). Since low-energy work[19] on Pb^{207} suggests that the level spacing in this isotope[20] is rather small ($\sim$10 kev), it is not expected that we would resolve very well the Pb^{207} resonances in either sample. It is, however, possible to determine the average contribution to the total cross section due to Pb^{207} resonances. The contribution due to neutrons of angular momentum l is given[21] approximately by $\bar{\sigma}_{C.N.}=2\pi^2\lambda^2E^{\frac{1}{2}}(2l+1)v_l(\Gamma_n^{(l)}/D)f\cos2\alpha_l$, where f is the isotopic abundance ($\sim$25%) and α_l is the potential phase shift. In the neighborhood of lead the s-wave strength function is known[22] to be less than 1.0×10^{-4}. Thus $\bar{\sigma}_{C.N.}(Pb^{207})<0.08$ barn everywhere in this energy range. Similarly if Pb^{207} has about the same p-wave strength function as we obtain in this paper for Pb^{208} (i.e., $\simeq0.5\times10^{-4}$), the p-wave contribution due to resonances in Pb^{207} is <0.07 barn everywhere. Thus the total resonance contribution due to Pb^{207} in either sample is <0.15 barn. Similarly, in the natural lead sample the average contribution due to resonances in Pb^{206} is <0.15 barn. Since the spacings and width in Pb^{206} are expected to be larger, these resonances should not be averaged out completely and should still be observable. This is easily seen in Figs. 4 and 5. Since the error in our absolute cross sections is roughly ±0.5 barn, it is not worthwhile to try to take account of this averaged contribution (<0.3 barn for natural lead, and <0.15 barn for compensated lead). In our analysis here we shall therefore be interested only in the "obvious" resonances at $E_n\simeq352$, 526, and 718 kev, and, as we shall see later, in the "hidden" resonance at $E_n=515$ kev.

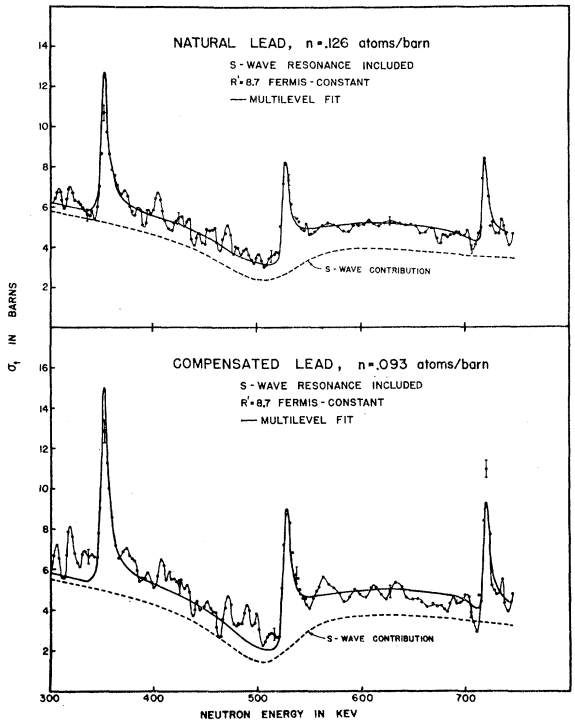

FIG. 5. σ_t for natural and compensated (for Pb^{206}) lead. The solid line shows in each case the fit obtained by including the s-wave resonance at 515 kev with the parameters listed in Table III. The contribution of the three p-wave resonances in this fit as well as in the fits shown in Fig. 4 was calculated by the use of a Bethe-type multilevel expression.

TABLE III. Resonance parameters for Pb^{208}.

E_0 (kev)	Γ_n (kev)	Γ_n (kev)	$\Gamma_n^{(l)}$ (ev)	$10^3\times\gamma_\lambda^2/(\gamma^2)_{s.p.}$
352	6.45±1.3	6.96	21.1	6.720
515	···	100	141	44.90
526	7.1±1.5	6.15	13.0	4.140
718	5.7±1.0	4.86	8.0	2.548

The resonances at $E_n=352$, 526, and 718 kev all have σ_{max} greater than the theoretical maximum for statistical weight factor $g=1$ and therefore cannot be due to s-wave neutrons. The s-wave assignment is also ruled out by the fact that s-wave resonances in this energy region and for this large a potential scattering cross section should have inverted shapes, i.e., large dips followed by small peaks. Similarly $g=3$, and hence a d-wave nature, is ruled out because the resonances are wide enough so that with our resolution of $\simeq$2 kev to 4 kev we should see almost the full theoretical peak height. We have therefore attempted to analyze these resonances as $l=1$ ($g=2$) resonances.

In Table III Column 2 we list the parameters of these resonances as obtained by area analysis. We now attempt to fit the observed σ_t by varying the parameters within the limits assigned by area analysis.

Seth *et al.*[23] find $R'=9.5\pm0.2$ fermis at zero energy which corresponds to $\sigma_p(l=0)=7.15$ barns, at $E_n=300$ kev. This is much larger than required by our data, for which we find that $R'=8.7\pm0.2$ fermis gives the best fit. (This is not too disturbing since the value at zero energy is likely to be higher if a bound s-wave level exists close to zero energy.) Further we have assumed

[19] E. G. Bilpuch, K. K. Seth, C. D. Bowman, R. H. Tabony, R. C. Smith, and H. E. Newson, Ann. Phys. (to be published).

[20] It has become conventional in neutron physics to refer to the resonances in the cross sections of a target nucleus with atomic weight A as resonances in that nuclide while they actually correspond to excited states in the compound nucleus with atomic weight $(A+1)$. We will follow this convention in this paper.

[21] Kamal K. Seth, Can. J. Phys. **37**, 1199 (1959).

[22] D. J. Hughes, R. L. Zimmerman, and R. E. Chrien, Phys. Rev. Letters **1**, 1518 (1958).

[23] K. K. Seth, D. J. Hughes, R. L. Zimmerman, and R. C. Garth, Phys. Rev. **110**, 692 (1958).

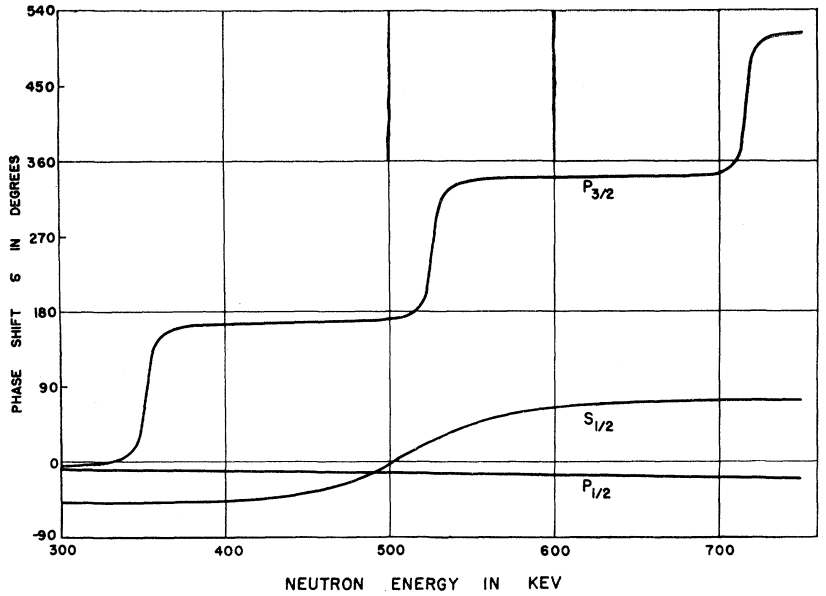

FIG. 6. Calculated phase shifts for Pb^{208}.

that $R=8.7$ fermis$=1.45\,A^{\frac{1}{3}}$ fermis, i.e., $R'/R=1.0$ and $\beta=(\sin^2\alpha_1')/(\sin^2\alpha)=0.4$,[24] since these values lead to the best fit shown in Fig. 6, and differ little from the theoretical result ($R'/R=1$, $\beta=0.5$ at $E_n=500$ kev) obtained by a simple square-well optical-model calculation[25] with $V_0=-42$ Mev, $\xi=0.03$, $r_0=1.45$ fermis.

Curves labeled (*a*) in Fig. 4 show attempts to fit the data by assuming $R'=8.7$ fermis (independent of energy) and only the three p-wave levels with parameters as listed in Table III. It is seen that the general level of the calculated curve is higher than that indicated by the data in the energy region 380 to 520 kev. It appears that R' itself is decreasing with energy. An attempt was therefore made to introduce a variation of R' with energy in such a way as to fit the data in this region. This called for variation of R' from 8.7 fermis at 300 kev to 4.7 fermis at 520 kev. This trend of R' was extrapolated up to 740 kev and the shape elastic scattering computed. The contribution from the p-wave levels, as calculated above was then added to it. The resulting fit is shown in Fig. 4, curves (*b*). Now, while the region up to 510 kev shows good fit, a large discrepancy appears in the higher energy region. The curves (*a*) and (*b*) considered together suggest that the s-wave contribution does indeed fall more rapidly than just shape-elastic scattering would predict in the region 300 kev to 520 kev, but apparently it returns to its normal shape-elastic scattering plateau again around 700 kev. This is precisely what the presence of an s-wave resonance in the neighborhood of 520 kev would do. Because of the large potential phase shift corresponding to $R'=8.7$ fermis, an s-wave resonance in this region will appear as a dip in the total cross section. A s-wave level was therefore postulated near 520 kev and its parameters were varied until a good fit was obtained to the natural Pb data. These parameters are listed in Table III and the fit is shown in Fig. 5. As a test of this hypothesis, without varying the parameters further, the cross sections were computed for compensated lead. The resulting fit is also shown in Fig. 5. It is found to be quite satisfactory. From the accumulated evidence we therefore conclude that the broad s-wave level does indeed exist and has the parameters $E_0=515\pm15$ kev, $\Gamma_n\simeq\Gamma=100\pm15$ kev.

In Fig. 6 we present the phase shifts corresponding to the fit shown in Fig. 5. Since from total cross-section data alone it is not possible to determine the absolute signs of the phase shifts, we have simply shown as a function of energy the total s-wave phase shift, the p-wave $p_{\frac{1}{2}}$ phase shift for shape elastic scattering, and the total $p_{\frac{3}{2}}$ phase shift.

DISCUSSION OF RESULTS

Carbon

The two independent methods used in the analysis of the carbon cross sections yield results which are in almost perfect agreement and hence lend strength to the validity of each method. The effective-range method yields a value of $\gamma_\lambda^2/E_\lambda$ without any assumption about the character of the bound levels—except that only one level is important. Specifying the energy of this level immediately gives γ_λ^2 but does not give the l value for this level. The other and more empirical method of fitting the observed cross section with a Breit-Wigner formula requires a definite assumption about the l value

[24] α_1' is the phase shift for p-wave shape elastic or "potential" scattering as defined by Feshbach *et al.* [H. Feshbach, C. E. Porter, and V. F. Weisskopf, Phys. Rev. **96**, 448 (1954)]. It differs from the pure hard-sphere scattering phase shift α_1 for p-wave neutrons in the averaged contribution of "far away" levels.

[25] H. Feshbach, C. E. Porter, and V. F. Weisskopf, Phys. Rev. **96**, 448 (1954).

and therefore lead to its assignment for the bound level. It is gratifying that the γ_λ^2 so obtained agrees well with that obtained from the effective-range theory. By specifying that the level responsible is at -1860 kev, we have obtained, with these two methods, the result that this level must have $l=0$, and $\gamma_\lambda^2=1.75$ Mev. Indeed we know that (d,p) stripping experiments[10,11] show that the level has $l=0$. However, we find that the reduced width of this level, according to McEllistrem's analysis of the (d,p) data,[11] is 0.83 Mev. This apparent discrepancy vanishes as soon as we realize that (d,p) reduced widths are very sensitive to the choice of the radius. McEllistrem uses $R=4.7$ fermis compared to our $R=3.3$ fermis. In terms of the Wigner limit our result is $\theta_\lambda^2\equiv\gamma_\lambda^2/(\gamma_\lambda^2)_{s.p.}=0.307$ while the value obtained from the (d,p) experiments is $\theta_\lambda^2=0.295$.

Calcium

Our results for calcium reveal a rather rapid variation of $(\bar{\Gamma}_n^0/D)$ with energy. Figure 7 shows that while the spacing remains essentially constant over the energy region 0 to 600, $\bar{\Gamma}_n^0$ increases rather rapidly so that for the first five resonances up to 230 kev $(\bar{\Gamma}_n^0/D)=(1.1\pm0.7)\times10^{-4}$, for the 9 resonances up to 400 kev $(\bar{\Gamma}_n^0/D)=(2.6\pm1.3)\times10^{-4}$, and for the 12 resonances up to 630 kev $(\Gamma_n^0/D)=(3.4\pm1.3)\times10^{-4}$. The increase of Γ_n^0 with energy is usually indicative of gradually worsening resolution resulting in a lumping together of groups of resonances. While this can hardly affect our conclusion about the variation of $(\bar{\Gamma}_n^0/D)$ with energy, it is of importance as far as average spacing is concerned. The rather constant slope of the solid line histogram in Fig. 7 is usually interpreted as indicating that the level resolution capability of the instrument is constant over this energy range. It does not, however,

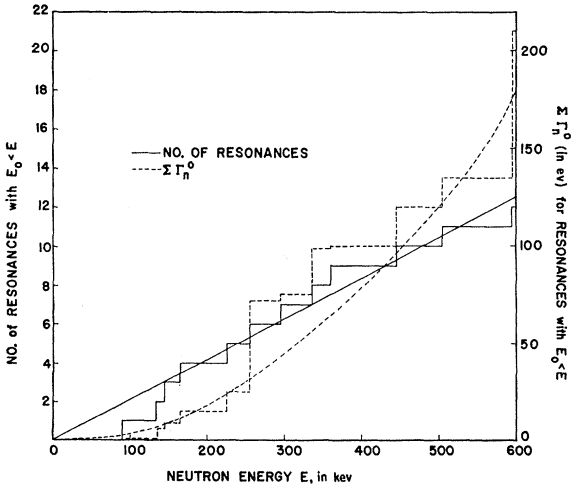

FIG. 7. The solid line histogram (scale at the left) corresponds to the total number of levels in Ca^{40} below a given energy, and the dashed line histogram (scale at the right) corresponds to $\Sigma\Gamma_n^0$ for levels below a given energy. The solid and dashed curves are drawn only to indicate the general trend of the histogram plots.

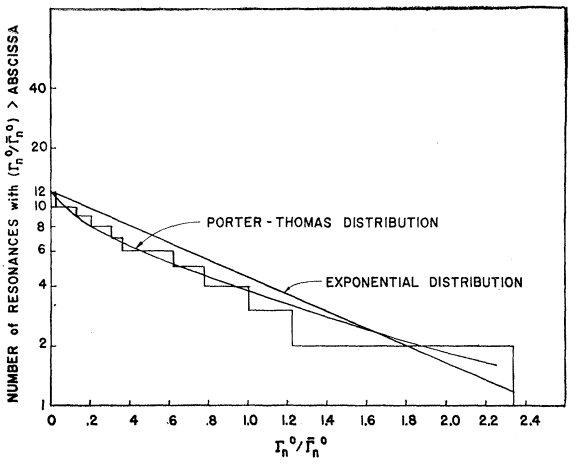

FIG. 8. Distribution of level widths in Ca^{40}. The histogram shows the total number of levels with $(\Gamma_n^0/\bar{\Gamma}_n^0)\geqslant$ abscissa. The curves pertain to calculated frequency for an exponential distribution function, $\exp(-\Gamma_n^0/\bar{\Gamma}_n^0)$ and to the Porter-Thomas distribution function $(2\pi\Gamma_n^0/\bar{\Gamma}_n^0)^{-\frac{1}{2}}\exp(-\Gamma_n^0/2\bar{\Gamma}_n^0)$. The Porter-Thomas distribution gives the better agreement.

rule out the possibility that a constant fraction of small levels are missed over the entire range because of the resolution being equally poor at all energies. A plot of the distribution of $(\Gamma_n^0/\bar{\Gamma}_n^0)$ is, however, capable of furnishing information about missing levels. Figure 8 shows such a plot. Not only does it show that no appreciable number of small levels are being missed, but it indicates also that the resolution is sufficiently good so that the data differentiate between distribution functions. The Porter-Thomas distribution[26] is preferred over the exponential. The latest calculation of Feshbach[27] for the strength function at zero energy with a rounded edge optical potential predicts a value 1.2×10^{-4}. K^{39} as well as Ca^{40} are found to have a value 1.1×10^{-4} in the 0–200 kev region. It would be of interest to determine whether the K^{39} strength function also shows an increase with energy like Ca^{40}. It is found that the required energy dependence of the Ca^{40} strength function can be obtained from a square well optical model calculation. However, in these calculations it is found that $(\bar{\Gamma}_n^0/D)$ increases as R' decreases. It does not appear possible to obtain R' relatively independent of energy and $\bar{\Gamma}_n^0/D$ varying rather rapidly with energy. It is well known though, that rounding the potential well does decouple the variations of these two parameters. Conceivably such calculations might explain our empirical observation. It has also been pointed out recently that near magic neutron and proton numbers the optical well parameters undergo sudden changes.[28] It would perhaps be worthwhile to seek

[26] C. E. Porter and R. G. Thomas, Phys. Rev. **104**, 483 (1956).
[27] H. Feshbach, in *Nuclear Spectroscopy* (Academic Press, New York, 1960), Part B, p. 1058.
[28] Atsushi Sugie, Phys. Rev. Letters 4, 286 (1960).

an answer to our question in the shell model effects on the optical model parameters.

Lead

It appears that the proposed explanation of the behavior of the Pb^{208} cross sections in the neighborhood of 515 kev does indeed provide an excellent fit to the cross sections observed. While it may be debatable whether two levels of the same spin and parity can exist within their half-width and still be amenable to the usual resonance theory, there is no theoretical objection to the situation we observe in Pb^{208}. The $\frac{3}{2}^-$ level can certainly exist within the half-width of the $\frac{1}{2}^+$ level. It is true that the $\frac{1}{2}^+$ level required is unusually wide compared to the other resonances in Pb^{208}. However, in terms of the Wigner limit it is only about 5% of the single-particle width. For a double magic nucleus with very large spacing this is entirely possible.

ACKNOWLEDGMENT

The authors wish to acknowledge the generous help of the entire Van de Graaff group at Duke, and especially the cooperation and help of Dr. P. R. Bevington, Mr. R. J. Rummel, and Mr. W. Rolland in the development and design of this experiment. The support of the National Science Foundation under whose auspices some of the calculations were performed on the Duke University IBM-650 computer is also gratefully acknowledged. We also wish to thank Miss Dorothy Brand for help in numerous computations.

PHYSICAL REVIEW VOLUME 121, NUMBER 4 FEBRUARY 15, 1961

Decay of 16-Minute Ta^{182m}†

A. W. SUNYAR
Brookhaven National Laboratory, Upton, New York

AND

P. AXEL*
Physics Department, University of Illinois, Urbana, Illinois

(Received July 5, 1960)

A revised decay scheme of the 16-minute isomer Ta^{182m} involves three states of Ta^{182} at excitation energies of 147 kev, 319 kev, and 503 kev. Transition multipolarities were classified by measuring both gamma-ray coincidences and internal conversion electrons. The 503-kev isomeric state decays mainly (98%) by a 184-kev $E3$ transition to the 319-kev state. This 319-kev state decays mainly (94%) to the 147-kev state by means of a 172-kev transition that is predominantly $M1$. The 147-kev transition to the ground state is also predominantly $M1$. Two of the three possible crossover transitions were observed; a 356-kev $M4$ transition originates at the isomeric level and a 319-kev $E2$ transition connects the second excited state with the ground state.

The 147-kev and the 319-kev states are probably the first and second excited rotational states of the ground-state configuration. The relevant rotational parameters are of particular interest because very little is known about moments of inertia for odd-odd nuclei.

The relative probabilities were determined for pile neutron activation of the 16-minute isomer, Ta^{182m}, and the 112-day ground state, Ta^{182}. If the ground-state formation cross section is taken as 21 barns, the corresponding value for the isomer is only 9 mb.

INTRODUCTION

THE 16-minute Ta^{182m} activity was first reported by Seren, Friedlander, and Turkel,[1] who measured the slow-neutron activation cross section as 34±7 mb. The first preliminary energy measurement was made by Hole,[2] who assigned 180±7 kev to the isomeric transition after studying the conversion electrons in a magnetic spectrometer. The $E3$ classification[3] of the isomeric transition was based on the lifetime, the ratio of internal conversion coefficients,[2] and the K-shell conversion coefficient.[4]

We first re-examined the decay of 16-minute Ta^{182m} to search for a direct beta-decay branch to W^{182}, the daughter of the beta-decaying 112-day ground state, Ta^{182}. (No 16 minute beta branch was ever found. The experiments would have been quite sensitive to high-energy beta rays from Ta^{182m} to levels near the ground state of W^{182}, but it is difficult to estimate the sensitivity to low-energy beta rays.)

During these measurements, our coincidence scintillation studies uncovered two cascade gamma rays with

† Work performed under the auspices of the U. S. Atomic Energy Commission.

* Summer Visitor at Brookhaven National Laboratory, Upton, New York, when this work was begun.

[1] L. Seren, H. N. Friedlander, and S. H. Turkel, Phys. Rev. **72**, 888 (1947).

[2] N. Hole, Ark. Mat. Astron. Fysik **36A**, No. 9 (1948).

[3] M. Goldhaber and A. W. Sunyar, Phys. Rev. **83**, 906 (1951).

[4] A. W. Sunyar, Phys. Rev. **83**, 864 (1951).